Journal of Electroanalytical Chemistry 790 (2017) 1–10

Contents lists available at ScienceDirect

Journal of Electroanalytical Chemistry

journal homepage: www.elsevier.com/locate/jelechem

Electrochemical determination of fisetin using gold electrodes modified with thiol self-assembled monolayers

Eliana Maza, Héctor Fernández, María Alicia Zon *, Marcela Beatriz Moressi *

Grupo de Electroanalítica (GEANA), Departamento de Química. Facultad de Ciencias Exactas, Físico-Químicas y Naturales. Universidad Nacional de Río Cuarto, Agencia Postal No 3 – 5800 - Río Cuarto, Córdoba, Argentina

ARTICLE INFO

Article history:
Received 2 November 2016
Received in revised form 14 February 2017
Accepted 16 February 2017
Available online 02 March 2017

Keywords:
Flavonoid
Fisetin
Self-assembled monolayers
Cyclic voltammetry
Square wave voltammetry

ABSTRACT

The electro-oxidation of fisetin (FIS) at gold electrodes modified with self-assembled monolayers (SAM) is studied in 15% dimethylsulfoxide + 85% phosphate buffer solutions of different pH using cyclic and square wave voltammetries. Gold electrodes were modified with 2-mercaptoethanesulfonic acid (2-MES) and 4-mercaptophenol (4-MP). Both modified electrodes were characterized by reductive desorption, electrochemical impedance spectroscopy, contact angle measurements, and by the determination of the apparent surface pKa. The FIS first oxidation peak showed an electrode process controlled by diffusion at 2-MES modified gold electrodes, while the electrode process showed a diffusion/adsorption mixed control at 4-MP modified gold electrodes. Square wave voltammetry was used to perform the FIS quantitative determination at both modified electrodes using the commercial reagent. Calibration curves were linear in the concentration range from 1×10^{-7} to 1×10^{-4} M and from 1×10^{-6} to 1×10^{-5} M for 2-MES and 4-MP SAM modified electrodes, respectively. Limits of detection for a 3:1 signal to noise ratio were 5×10^{-8} M (14.3 ppb) and 5×10^{-7} M (143 ppb) for 2-MES and 4-MP modified electrodes, respectively. The reproducibility and the repeatability were 2.2% and 0.5% for 2-MES SAM modified electrodes, and 1.6% and 1.3% for 4-MP SAM modified electrodes, respectively.

1. Introduction

Flavonoids are a large group of substances widely distributed in the plant kingdom [1]. They have the general structure of a carbon skeleton, which contains two phenyl rings and a heterocyclic ring [1]. Flavonoids exhibit anti-cancer, anti-inflammatory and anti-viral properties, as a result of their antioxidant activities [2]. Fisetin (3,3′,4′,7-tetrahydroxyflavone, FIS, Fig. 1) is a flavonoid that has attracted significant attention, due to its wide spectrum of biological activities. Particularly, FIS produces apoptosis of cancer cell [3], suppresses inflammatory processes in most human cells [4], inhibits platelet aggregation induced by thrombin and cathepsin G [5], and acts as free radical scavenger [6]. FIS produces inactivation of protein kinase C and HIV-1 protease enzymes, which is required to develop the HIV virus [7], and inhibits non-enzimatic glycosylation of hemoglobin [8]. FIS can also improve memory in patients with memory disorders [9].

Chromatographic methods are the most used to quantify flavonoids, mainly HPLC with different types of detectors [10–12]. Stripping voltammetry at a carbon paste electrode coupled to a flow injection system has been used for the simultaneous determination of flavonoids including FIS [13].

However, studies related to the basic electrochemical behavior of flavonoids are scarce [14–17]. Hodnick et al. [14] studied FIS electrochemical oxidation at glassy carbon electrodes in 15% dimethylsulfoxide (DMSO) + pH 7.00 phosphate buffer solutions (PBS). These authors found a complex electro-oxidation mechanism, where the first oxidation peak corresponds to a quasi-reversible process, involving $2e^-$ and $2H^+$. Hendrickson et al. [15,16] studied the electrochemical oxidation of quercetin, luteolin and FIS at glassy carbon electrodes in ethanolic solutions. They also found a complex electro-oxidation mechanism, where all flavonoids which have a catechol group in the B ring show a quasi-reversible oxidation peak at low potentials, which corresponds to the transfer of $2e^-$ and $2H^+$.

We studied the FIS first electrochemical oxidation at glassy carbon electrodes in 15% DMSO + pH 4.00 phosphate buffer solution, and found that the first oxidation peak corresponds to a quasi-reversible redox process involving $2e^-$ and $2H^+$, which showed a diffusion/adsorption mixed control. The adsorption process was studied in blank solutions, and it was found that the Frumkin adsorption isotherm was the best to describe the specific interaction of FIS with carbon electrodes. Also, a full thermodynamic and kinetics characterization of the surface redox couple was carried out by square wave voltammetry (SWV) [18].

* Corresponding authors.
E-mail addresses: azon@exa.unrc.edu.ar (M.A. Zon), mmoressi@exa.unrc.edu.ar (M.B. Moressi).

http://dx.doi.org/10.1016/j.jelechem.2017.02.030
1572-6657/

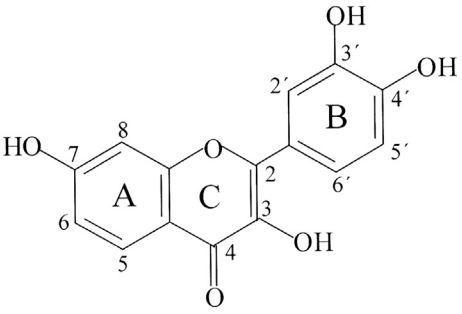

Fig. 1. Chemical structure of fisetin.

Gold electrodes modified with self-assembled monolayers (SAM) have gained much attention in last year's because of their easy preparation, excellent properties and diverse applications in various fields of science [19–22]. These modified electrodes are used as sensors and as a base for the construction of biosensors for analytical applications [23,24]. SAM modified electrodes control the solid/liquid interface, can increase the selectivity and sensitivity, and decrease response times and overpotentials [25–27]. This behavior arises from the direct blocking of the electrode surface to the access of substances, inhibiting some processes, and favoring others [19]. It was demonstrated that the electrochemical response of various substrates has widely been improved at these SAM modified electrodes [25,26]. These modified electrodes have also been used to study surface organic reactions [28], modeling cell membranes [29], and as a model surface for studying materials/blood interactions to develop biomedical devices [30].

In this work, we study the FIS electro-oxidation at SAM modified gold electrodes in 15% DMSO + 85% PBS of different pH by cyclic (CV) and SWV voltammetries. Gold electrodes were modified with 2-mercaptoethanesulphonic acid (2-MES) and 4-mercaptophenol (4-MP). The FIS electrochemical behavior at both modified and bare gold electrodes is compared. Both SAM modified electrodes were characterized by reductive desorption, electrochemical impedance (EI) spectroscopy, contact angle measurements, and by the determination of the apparent surface pKa. The FIS quantitative determination was carried out at both modified electrodes through calibration curves obtained from SWV measurements using the commercial reagent.

2. Experimental

2.1. Reagents

FIS, 2-MES, 4-MP and dodecanethiol (DDT) were purchased from Sigma-Aldrich. Buffer solutions were prepared by mixing different volumes of 0.5 M NaH_2PO_4 and 0.5 M Na_2HPO_4 (both Merck, p.a.) aqueous solutions. KNO_3 and KCl were Merck p.a. Water was purified by a Labconco WaterPro Mobile System, Model 90901-01. Stock solutions 1×10^{-3} M FIS were prepared in DMSO (Merck, p.a.), and kept in the refrigerator. Working solutions were prepared daily by adding different aliquots of the stock solution to 15% DMSO + 85% PBS of different pH. All reagents were used as received.

2.2. Apparatus and experimental measurements

CV and SWV experiments were performed using an AutoLab PGSTAT 12 potentiostat, controlled by the GPES 4.9 electrochemical software, from Eco-Chemie, Utrech, The Netherlands. Electrochemical measurements were carried out in a two-compartment Pyrex cell. The working electrode was a polycrystalline gold disk of 1.6 mm diameter obtained from BAS (USA). The gold disk was polished successively with wet alumina powder (0.3 and 0.05 μm, from Fischer). Then, it was copiously rinsed with distilled water and sonicated in a water bath during 2 min. Polished electrodes were then pretreated by cycling the potential between 0.3 and 1.7 V at 0.1 V s^{-1} in 0.5 M H_2SO_4 aqueous solution until the characteristic cyclic voltammogram for a clean gold electrode was obtained [31]. Electrodes were then rinsed with water and ethanol. The gold disk microscopic area was obtained from the charge of the reduction oxide stripping peak in sulphuric acid aqueous solutions by using the accepted 430 μC cm^{-2} ratio [32]. An average microscopic area of (0.12 ± 0.02) cm^2 was calculated from three replicated measurements. SAM were prepared by immersing the pretreated electrode in a 1×10^{-2} M stirred ethanolic solution during a given modification time (t_{mod}), which was varied from 5 to 60 min. After modification, the electrode was washed with ethanol and water.

The counter electrode was a platinum foil of large area (A ≅ 2 cm^2). An aqueous saturated calomel electrode (SCE) or pseudo-reference silver wires were used as reference electrodes. Solutions were deoxygenated by bubbling pure nitrogen during at least 10 min prior to the measurements.

Measurements of pH were performed with an Orion 8104 Ross Combination electrode connected to an Orion Model 720A pH-meter, which was calibrated daily with commercial buffers.

Experiments were performed at 25.0 ± 0.2 °C.

The scan rate (v) in CV was varied from 0.025 to 0.600 V s^{-1}. Parameters of SWV were: the amplitude ($\Delta E_{SW} = 0.025$ V), staircase height ($\Delta E_S = 0.005$ V), and the frequency (f = 20 Hz).

EI spectroscopy experiments were carried out using an AutoLab PGSTAT 30 potentiostat controlled by the FRA impedance software These measurements were performed in 1×10^{-3} M $[Fe(CN)_6]^{-4/-3}$ + 0.1 M KCl aqueous solutions. The applied dc potential was 0.190 V vs. SCE, which corresponds to that of the formal potential of the redox couple. The amplitude of sine wave perturbation was 5 mV. The frequency was in the range from 0.1 Hz to 10 kHz. The experimental Nyquist plots (out-of phase, Z″ vs. in phase, Z′ impedance components) were fitted using the FRA electrochemical impedance software incorporated to the AutoLab PGSTAT 30 potentiostat.

The contact angle measurements were performed using an Intel Play QX3 which has a 60× objective. The images were analyzed with the Image I (plugins DROP ANALYSIS) software.

3. Results and discussion

3.1. Characterization of SAM

We have carried out a characterization of 2-MES and 4-MP monolayers to explain the different electrochemical behavior of the FIS first oxidation peak at both modified electrodes. For comparison, we also characterize the monolayer formed by the DDT at gold electrodes, which it is well known to form a compact and tidy monolayer [19].

Thus, we studied the reductive desorption of monolayers in 0.5 M KOH, which allows to determine the monolayer coverage. Potential sweeps at sufficiently positive or negative potentials cause desorption of thiol [19], producing sulfoxy or thiolate anions, respectively [33,34]. Studies related to the monolayer desorption allow to obtain information about the stability and packing density of the monolayer [35].

In addition, we characterize monolayers through electrochemical impedance spectroscopy, contact angle measurements, and the determination of the apparent surface pKa for 2-MES and 4-MP monolayers.

3.1.1. Reductive desorption

When SAM modified gold electrodes are immersed in 0.5 M KOH, and the potential is swept towards negative potentials, one or two reduction peak/s can be observed [36]. The reductive desorption reaction of the thiolate is well known [19].

Fig. 2 shows cyclic voltammograms obtained for the reductive desorption of SAM formed by 4-MP, 2-MES and DDT. Two desorption peaks were found for 4-MP and 2-MES SAM (Fig. 2a and b, respectively). The presence of different crystallographic domains at polycrystalline gold electrodes is well known [37]. On the other hand, only one

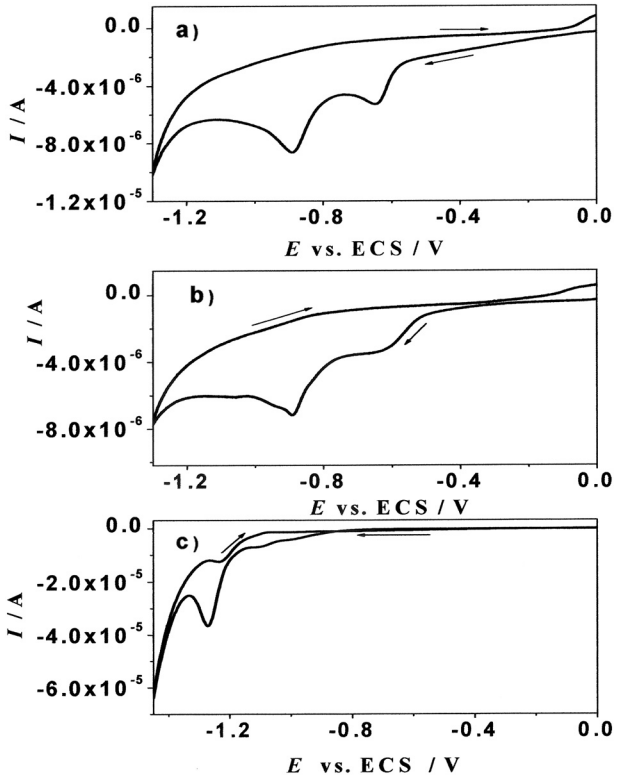

Fig. 2. Cyclic voltammograms recorded for the reductive desorption of thiols in 0.5 M KOH. a) 4-MP, b) 2-MES and c) DDT. $t_{mod} = 60$ min. $v = 0.100$ V s^{-1}.

desorption peak was found for DDT SAM (Fig. 2c). This behavior is expected when interactions between SAM and the gold electrode surface is strong. The position and shape of peak/s of desorption give an indication of the stability and compactness of monolayers [19].

From the reductive charge (Q_{red}) of desorption peak/s, we calculated Γ_{red} of 2-MES, 4-MP and DDT SAM through Eq. (1) [38]:

$$\Gamma = \frac{Q}{n\ F\ A} \quad (1)$$

where $\Gamma = \Gamma_{red}$ is the surface coverage, $Q = Q_{red}$, n is the exchanged electron number, $n = 1$ [19] and F is the Faraday constant.

Table 1 shows values of Q_{red}, Γ_{red} and peak potentials ($E_{p,1}$ and $E_{p,2}$ for the first and second reduction peaks, respectively) obtained from the reductive desorption of the different SAM.

From these results, Γ_{red} of all monolayers are very close to that expected for a compact monolayer, i.e., 7.7×10^{-10} mol cm^{-2} [19], which would indicate that thiol adsorbed molecules would be in a perpendicular direction to the electrode surface [20,39].

3.1.2. Electrochemical impedance spectroscopy

EI spectroscopy allows to evaluate the capability of blocking of a SAM, the presence of pinholes and/or defects, and to determine its disorder degree [40].

Table 1
Parameters obtained from the reductive desorption of SAM of different thiols in 0.5 M KOH aqueous.

SAM	Q_{red}/μC	$10^{10}\Gamma_{red}$/mol cm^{-2}	$E_{p,1}/E_{p,2}$/V
4-MP	7.8	6.2	−0.64/−0.89
2-MES	9	7.2	−0.62/−0.89
DDT	12	9.5	−1.27

Fig. 3 shows Nyquist plots for the bare electrode, and DDT, 2-MES and 4-MP modified electrodes. Thus, a plot of Z″ vs. Z′ was linear for the bare gold electrode, with unit slope (Fig. 3a), showing a diffusion controlled electrode process (Warburg impedance) [38]. Moreover, a semi-circle was found throughout of all frequency range studied for the DDT modified gold electrode (Fig. 3b), which corresponds to a process limited by charge transfer. It is well known that longer chain thiols, and without functional groups exposed to the electrolytic solution generate more compact and organized monolayers.

For 2-MES and 4-MP SAM (Fig. 3c and d, respectively) the behavior is similar to that found for the bare gold electrode, and can be explained by considering the overlapping of the diffusion layer as a result of the closeness of pinholes and/or defects present in these SAM [41]. This behavior also indicates that the charge transfer between 2-MES and 4-MP modified gold electrodes and the probe redox probe is diffusion controlled.

The equivalent circuits which describe this behavior are shown in Scheme 1. For the bare electrode, and 2-MES SAM and 4-MP SAM modified electrodes, the best fitting was obtained with the equivalent circuit of Scheme 1a, where CPE and R_s represent the constant phase element and the resistance of the solution, respectively. R_{ct} and W are the charge transfer resistance and Warburg impedance, respectively. On the other hand, the experimental data for the DDT SAM modified gold electrode were better fitting using the equivalent circuit described by the Scheme 1b, where R_{SAM} is the charge transfer resistance due to the presence of the SAM, which is associated with the movement of water and ions within the layer in response to ac perturbation.

The thiol chemical structures can explain the different behavior found for these modified electrodes. Thus, the 2-MES SAM does not offer a significant resistance to charge transfer as a result that 2-MES is a short chain thiol. Moreover, the 4-MP SAM has a high conductivity due to delocalization of π electrons of the aromatic ring, producing a low resistance to charge transfer [42]. On the contrary, as it was previously described the monolayers obtained by DDT are more compact and tidy [19].

Assuming that all of faradaic current of the redox probe is due to its discharge at SAM defects is possible to obtain the SAM surface coverage (θ_{SAM}) through the following equation [39]:

$$\theta_{SAM} = 1 - \frac{R_{ct,Au}}{R_{ct,SAM}} \quad (2)$$

where $R_{ct,Au}$ and $R_{ct,SAM}$ are the resistances to the charge transfer at the bare gold and SAM modified electrodes, respectively. Values of $R_{ct,Au}$ and $R_{ct,SAM}$ were obtained from the fitting of impedance spectra using the equivalent circuits shown in the Scheme 1.

Values obtained per unit area from the best fitting are shown in Table 2. Values of σ vary between 0 and 1. σ is related to the angle of rotation of a capacitive transmission line on the complex plane plots. A value of $\sigma = 1$ indicates that the behavior of CPE is equal to an ideal capacitor [41], while values of σ less than unity suggest a structural disorder of the monolayer [43,44]. Values of σ between 0.95 and 0.97 indicate that SAM has a small number of pinholes. Based on σ values (Table 2), the increasing degree of ordering of SAM would be 2-MES < 4-MP < DDT. In addition, the impedance of the CPE is given by [45]: $Z_{CPE} = 1/Q_{CPE}(j\omega)^{\sigma}$, where Q_{CPE} is a constant in $\Omega^{-1}\ cm^{-2}\ s^{\sigma}$, $j = (-1)^{1/2}$ and ω the angular frequency ($\omega = 2\pi f$). Q_{CPE} values obtained were in the following order: DDT < 4-MP < 2-MES (Table 2).

In addition, the R_{ct} increases in the following order: bare Au electrode < 4-MP < 2-MES < DDT [41]. On the other hand, the solution resistance (R_s) is independent of modifications of the electrode surface [45]. Thus, values of R_s obtained from the fitting of experimental data were almost constant for bare and modified electrodes. An average value of $R_s = (1.8 \pm 0.7)$ kΩ cm^{-2} (26 ± 4) Ω cm^2 was calculated. In addition, the same value of the Warburg impedance $(182 \pm 7) \times 10^{-6}\ \Omega^{-1}\ s^{1/2}$

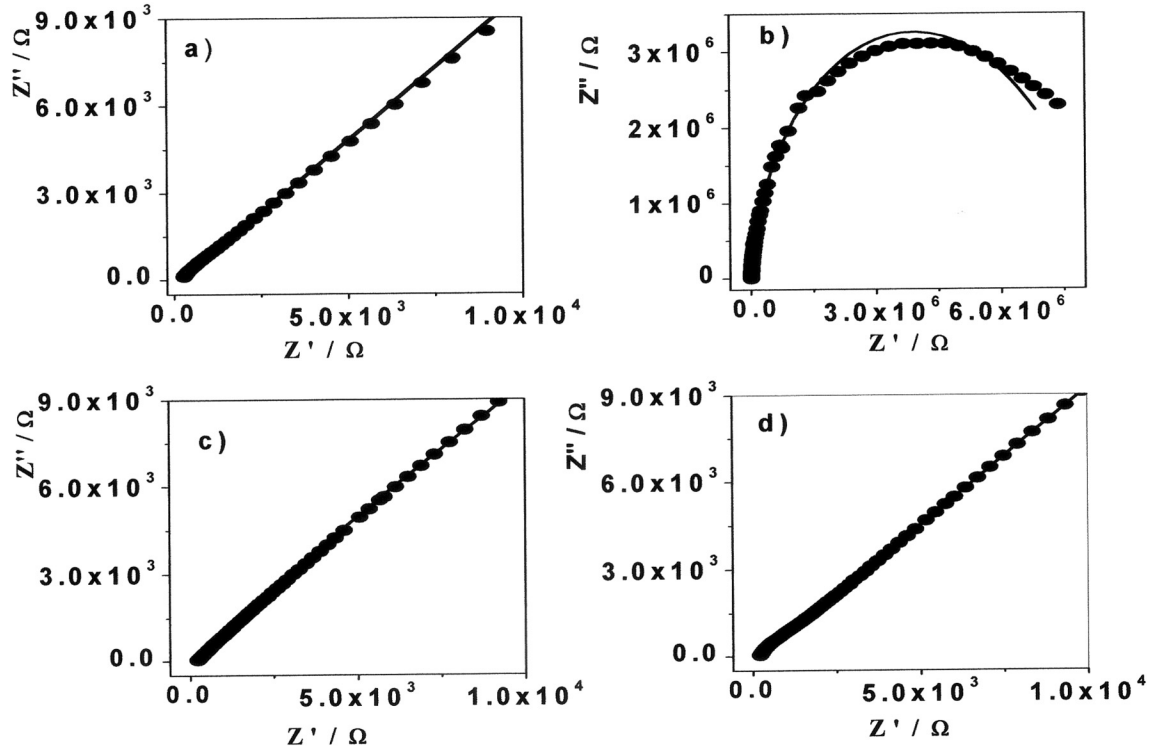

Fig. 3. Experimental (●) and theoretical (solid line) Nyquist plots recorded for a) the bare gold electrode, b) DDT, c) 2-MES and d) 4-MP SAM modified electrodes in 1×10^{-3} M of $[Fe(CN)_6]^{-4/-3}$ in 0.1 M KCl. $t_{mod} = 60$ min. Frequency range: 0.1 Hz to 10 kHz. Applied dc potential = 0.190 V vs. SCE.

$(21.8 \pm 0.9) \times 10^{-6}\ \Omega\ cm^2\ s^{-1/2}$ was obtained for both the bare and SAM modified gold electrodes.

Moreover, different values were determined for the surface coverage ($\theta_{SAM,imp}$) of 2-MES, 4-MP and DDT SAM from Eq. 2. This behavior can be explained considering that only $\theta_{SAM,imp}$ of the SAM of aliphatic chains can be considered as surface coverage. On the contrary, values of R_{ct} of aromatic thiols also include currents transferred through π—π bonds, which produces low $\theta_{SAM,imp}$ as it was found for 4-MP SAM (Table 2). The order of $\theta_{SAM,imp}$ of aliphatic thiols was 2-MES < DDT, as expected considering the aliphatic chain length.

Moreover, higher values of σ correspond to lower values of Q_{CPE}, indicating that the more ordered SAM are also those more densely packed. In addition, bulky tail group with electrical charge produces a disorder of SAM by electronic repulsion [46].

3.1.3. Determination of apparent surface pK_a of SAM

The apparent surface pK_a of SAM is one important parameter to sense the SAM surface properties. The apparent surface pKa measures the acidity of the SAM, and the surface charge state at a given pH [47]. This parameter can be determined through various techniques, being the most simple the titration curve obtained from CV and contact angle measurements [47,48].

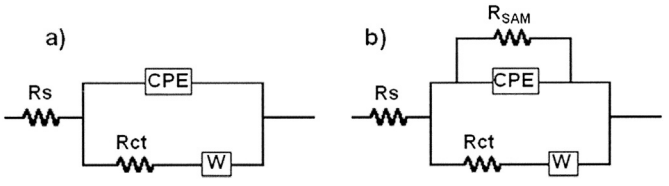

Scheme 1. Equivalent electrical circuits used to fit complex impedance plots for: a) bare and 2-MES and 4-MP SAM modified electrodes and b) DDT SAM modified electrode. R_s is the solution resistance; CPE is the constant phase element; R_{ct} is the electron transfer resistance; W is the Warburg impedance, and R_{SAM} is the monolayer resistance to ionic charge displacement through the film.

3.1.3.1. Cyclic voltammetry. This technique is based on the measurement of anodic peak currents, $I_{p,a,}$ from cyclic voltammograms of a simple redox couple as $[Fe(CN)_6]^{-4/-3}$, which is used as a probe molecule in aqueous solutions of different pH [47]. The electrochemical response of this simple redox couple is independent of pH at bare gold electrodes. However, the charge transfer between this simple redox couple and the electrode surface depends on the dissociation degree of the tail groups at a SAM modified electrode. Therefore, if AH is the tail acid group presents in a SAM, and considering the dissociation of a surface weak acid, the equilibrium can be described by [49]:

$$\Gamma_{AH} \quad \leftrightharpoons \quad \Gamma_{A^-} + \Gamma_{H^+} \tag{3}$$

The apparent surface Ka is defined by Eq. (4):

$$pK_a = pH + \log\frac{[\Gamma_{A^-}]}{[\Gamma_{AH}]} \tag{4}$$

where Γ_{A^-} and Γ_{AH} are the surface coverage's of the dissociated and non-dissociated forms of the SAM, respectively (the complete surface coverage of the monolayer is defined to be at unit concentration).

Assuming that the apparent total current (I) have contributions of both currents generated by the probe molecule at the SAM dissociated species (I_{A^-}) and the non-dissociated species (I_{AH}), and considering that $I = I_{A^-}\ [\Gamma_{A^-}] + I_{AH}\ [\Gamma_{AH}]$ and $[\Gamma_{A^-}] + [\Gamma_{AH}] = 1$, it is possible to obtain:

$$pK_a = pH + \log\frac{(I_{AH} - I_{A^-})}{(I - I_{A^-}) - 1} \tag{5}$$

where I_{A^-} and I_{AH} can be determined at high and low pH, respectively. Eq. (5) can be re-written as:

$$I = I_{A^-} + \frac{I_{AH} - I_{A^-}}{10^{pK_a - pH} + 1} \tag{6}$$

Table 2
Element values of equivalent circuits that best fit electrochemical impedance spectroscopy responses for both bare and SAM gold modified electrodes.

SAM	$Q_{CPE}/\mu\Omega^{-1}\,cm^{-2}\,s^{\sigma}$	σ	R_{ct} (kΩ cm^2)	R_{SAM} (kΩ cm^2)	χ^{2a}	θ_{SAM}
Bare gold	1.7 ± 0.4	1.0 ± 0.1	0.036 ± 0.002	–	0.008	–
2-MES	7.7 ± 0.4	0.76 ± 0.01	0.19 ± 0.01	–	0.026	0.806
4-MP	0.19 ± 0.08	0.89 ± 0.02	0.041 ± 0.002	–	0.028	0.123
DDT	0.035 ± 0.003	0.98 ± 0.02	36 ± 2	1.04 ± 0.03	0.267	0.999

[a] χ^2 is the chi square function. σ is defined in the text (Section 3.1.2).

Thus, a plot of I as a function of pH gives a sigmoid curve, with an inflexion point at a value equal to SAM apparent surface pKa.

Fig. 4 shows the variation of $I_{p,a}$, recorded for 1×10^{-3} M $[Fe(CN)_6]^{-4/-3}$ + 0.1 M KCl as a function of pH for 4-MP SAM (Fig. 4a), and 2-MES SAM (Fig. 4b).

The differential curve obtained for 4-MP SAM from fitting of experimental data is shown in the inset of Fig. 4a. A value of apparent surface $pK_a = 9.76$ was determined for 4-MP SAM. The apparent surface pKa of 2-MES SAM could not be determined (Fig. 4b), which indicates that tail group of this thiol is deprotonated at all pH values.

The charge transfer between the electrode surface and the redox couple is related to the charge of tail group of the thiol. Thus, the tail group of 4-MP SAM has no charge up to about pH 7.96. However, it is negatively charged as the pH increases, resulting in an electrostatic repulsion between the modified surface electrode and the probe molecule. This behavior leads to a decrease in current and an increase in the separation between the anodic and the cathodic peak potentials in cyclic voltammograms.

3.1.3.2. Contact angle measurements. The contact angle (γ) is defined as the angle formed between a solid surface and the tangent plane to a liquid surface, measured on the line of intersection [50]. The contact angle depends mainly on the cohesive forces that exist between the solid and the liquid. Thus, when the adhesive strength with the solid surface is very large in relation to the cohesive forces, the contact angle is <90° [51]. Contact angle measurements provide information about the composition and structures of the surfaces, mainly related to the hydrophobicity when the liquid used is water [52].

For SAM modified surfaces, contact angle measurements allow obtaining information about the wettability, thickness and the order degree of the SAM, and the polarity of the surface functional groups [19]. It is well known that for compact SAM of alkanethiols on Au(111) surfaces the contact angle in aqueous solution is 112°, while that for hydrophilic surfaces the angles are smaller than 15° [19].

When the hydrophobicity of the modified surface depends on the solution pH, it is possible to determine the apparent surface pKa through the pH of the intersection point.

The sigmoid curve is given by [53]:

$$\cos\gamma = \cos\gamma_{\Gamma_{AH}} + \frac{\cos\gamma_{\Gamma_{A^-}} - \cos\gamma_{\Gamma_{AH}}}{10^{pK_a - pH} + 1} \quad (7)$$

where $\cos\gamma_{\Gamma_{AH}}$ and $\cos\gamma_{\Gamma_{A^-}}$ are the cosines of contact angles of protonated and deprotonated forms of the surface monolayer, respectively.

Contact angle measurements were carried out at bare gold and both 2-MES and 4-MP SAM modified electrodes, using drops at different pH. The modified electrode was rinsed with water and then with the corresponding buffer solutions between measurements [53]. Fig. 5 shows the drop profiles obtained for the different electrodes tested. Contact angles for 2-MES SAM modified electrodes varied from 45° to 53° at different pH's, indicating that the monolayer chemical and structural properties are similar and independent of the pH. Contac angles for 4-MP SAM modified electrodes were of 41° for pH's 4–6. Then, the value decreased as the pH increased, reaching a value of 27° for pH's 12 and 13. This result indicates that the monolayer structural properties are pH dependent, and the monolayer presents an increase in hydrophilicity as the pH increases.

Fig. 6 shows the dependence of cos γ with the pH of drops for 4-MP SAM modified electrode (Fig. 6a) and bare and 2-MES SAM modified electrodes (Fig. 6b). The insert of Fig. 6a shows the corresponding differential curve. From the fitting of experimental data a value of 9.1 was determined for the apparent surface pK_a of 4-MP SAM modified electrode. On the other hand, the contact angle measurements showed no dependence with the pH of drops for both the bare and 2-MES SAM modified electrodes (Fig. 6b). These results are in very good agreement with those obtained by CV.

It is known that the apparent surface pKa of SAM with acid groups exposed to the electrolytic solution is higher than the pKa of the same thiol in solution [49]. The increase in apparent surface pKa can be attributed to the formation of intermolecular hydrogen bonds, being the protons strongly bonded to the electrode surface and making more difficult the deprotonation [47,49]. In addition, the deprotonation of an acid group in a SAM is thermodynamically unfavorable due to electrostatic repulsion of the ionized groups in the SAM/solution interface [39].

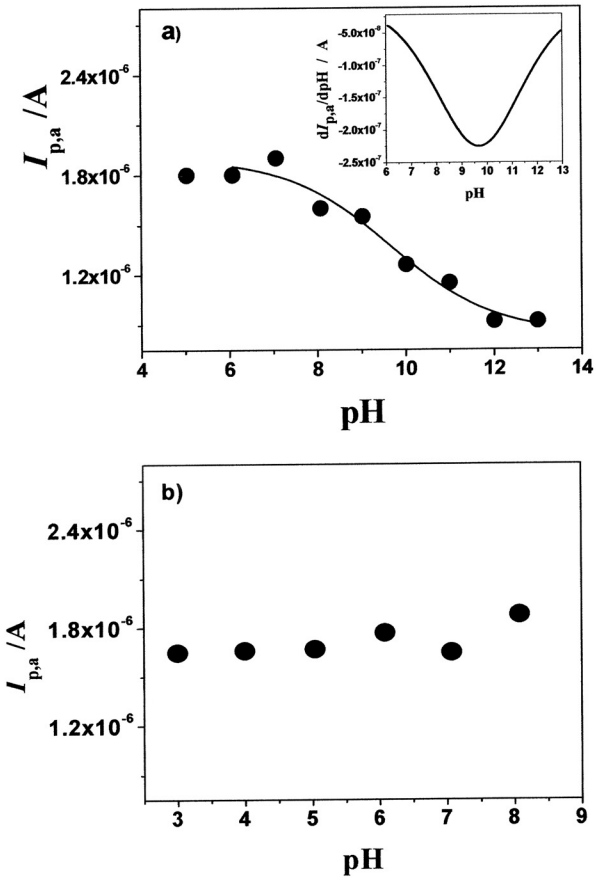

Fig. 4. Dependence of $I_{p,a}$ with the pH for 4-MP (a) and 2-MES (b) SAM modified electrodes in 1×10^{-3} M of $[Fe(CN)_6]^{-4/-3}$ redox couple in 0.1 M KCl. Experimental (●) and fitting (solid line) performed using Eq. (6). In the insert of Fig. 4a is shown the differential curve obtained from the fit of experimental data. t_{mod} = 60 min.

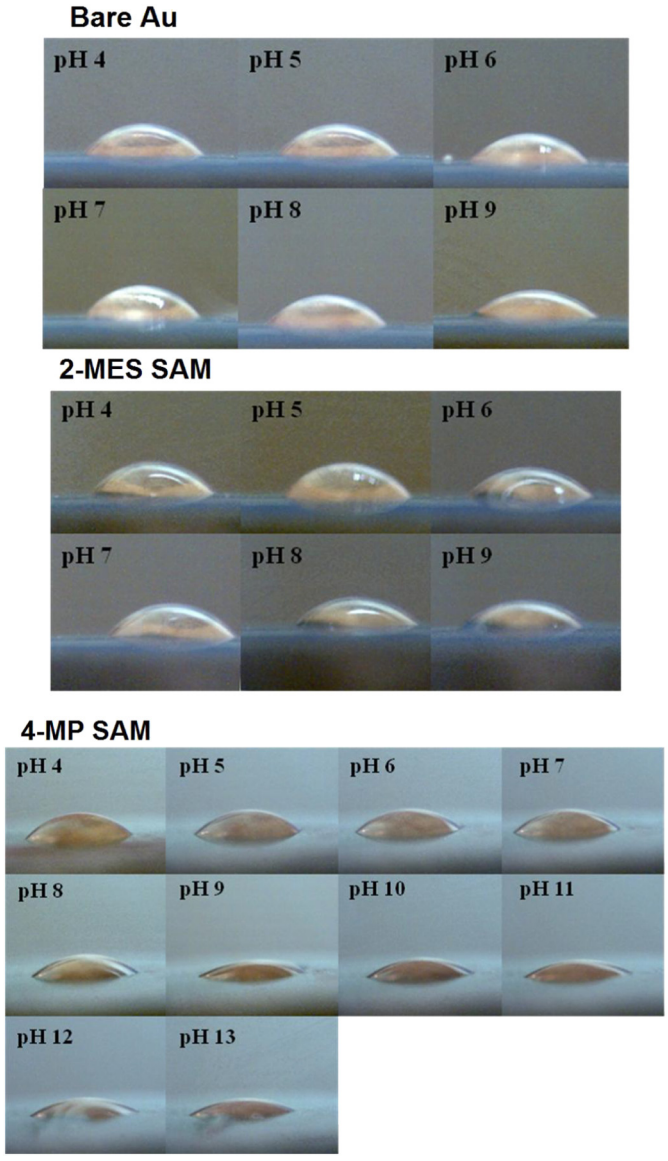

Fig. 5. Drop profiles obtained for both the bare gold and 4-MP and 2-MES SAM modified gold electrodes at different pH's.

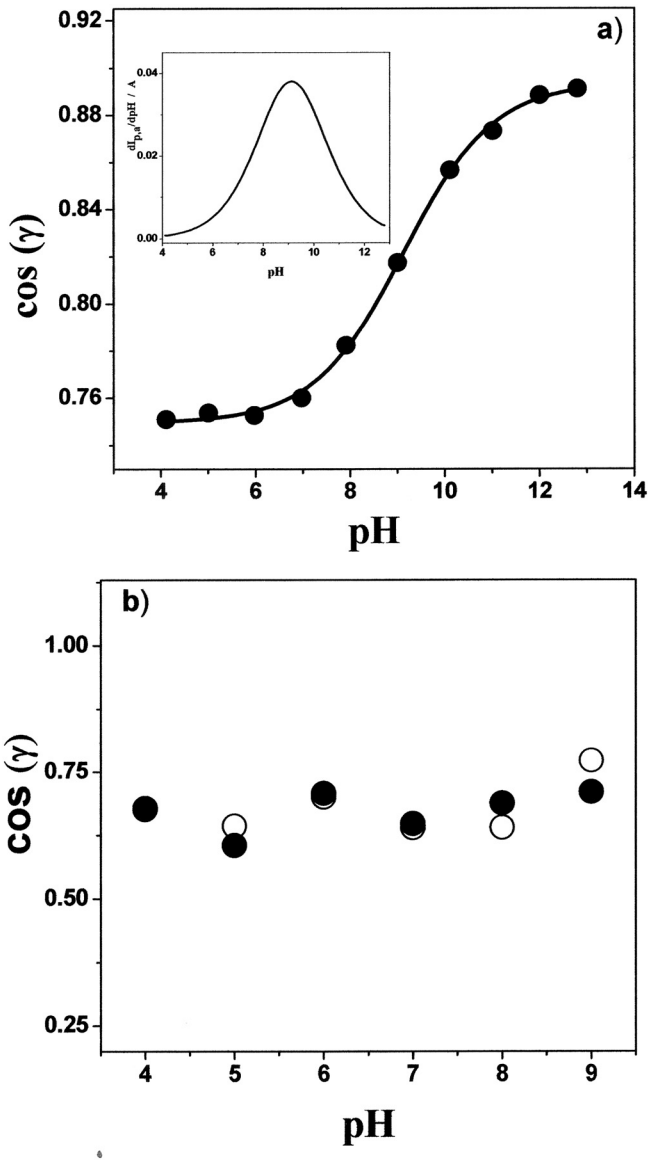

Fig. 6. Dependence of cos γ with the pH of drops for: a) (●) experimental and theoretical (solid line) values obtained for 4-MP SAM modified electrode. Insert of Fig. 6a shows the corresponding differential curve, and b) (o) bare and (●) 2-MES SAM modified electrodes.

On the other hand, the contact angles obtained for 2-MES SAM and 4-MP SAM are higher than those expected for a more compact and orderly monolayer [19]. This behavior also reflects a certain degree of disorder in these monolayers at all pH.

3.2. Electro-oxidation of FIS on bare gold electrodes

Fig. 7 shows cyclic voltammograms of FIS at a bare gold electrode in 15% DMSO + 85% pH 4.00 PBS. FIS shows a complex oxidation mechanism with three oxidation peaks identified as I, II and III, respectively. This behavior is similar to that previously reported at glassy carbon electrodes [15–18]. Peak I is the FIS main oxidation peak. It shows a quasi-reversible behavior, with an anodic peak potential ($E_{p,a}$) at about 0.340 V vs. SCE. It is well known that the charge transfer process for peak I corresponds to the oxidation of the 3′,4′-dihydroxy group in the B ring (Fig. 1), giving the corresponding quinone species as the main oxidation product [54]. An important feature of FIS cyclic voltammograms was that the $E_{p,a}$ of peak I was shifted to more positive potentials and its $I_{p,a}$ decreased significantly on successive scans (dash and dash dot lines in Fig. 7). This behavior suggests that the electrode is fouling by adsorption of FIS and/or its oxidation products.

We have previously discussed the nature of peaks II and III [18].

3.3. Electro-oxidation of FIS at gold electrodes modified with self-assembled monolayers

3.3.1. 2-MES SAM

Firstly, we studied the effect of the electrode modification time (t_{mod}) in the solution of 2-MES on FIS voltammetric responses. In spite of we found that voltammetric responses were practically independent of t_{mod}, short modification times (about 5 min) produced less reproducible voltammetric signals. However, a $t_{mod} \geq 60$ min allowed us obtaining a high reproducibility and repeatability in voltammetric responses. Thus, a $t_{mod} = 60$ min was chosen for subsequent experiments. This behavior could be explained considering that a longer t_{mod} allows a better organization of the SAM [19]. Under these experimental conditions, successive scans showed a slight decrease in the current

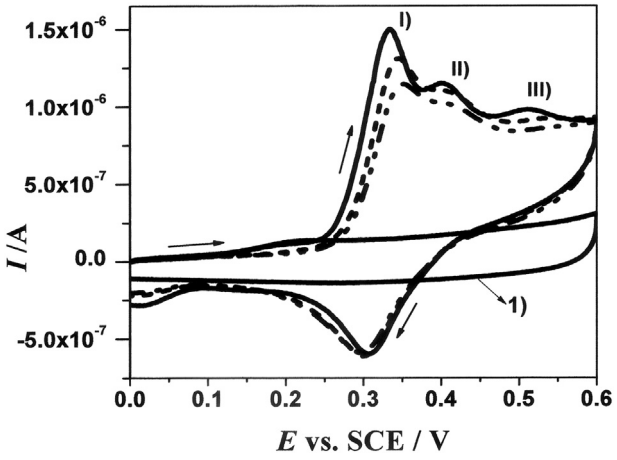

Fig. 7. Consecutive cyclic voltammograms of FIS in 15% DMSO + 85% pH 4.00 PBS at bare gold electrode (solid, dash, and dash dot lines are the first, second and the third scans, respectively). Line 1 is the cyclic voltammogram of the blank. $c^*_{FIS} = 1 \times 10^{-4}$ M. v = 0.050 V s^{-1}. Arrows indicate the direction of potential sweep.

only in the first two sweeps, and the voltammetric response was stabilized after the third sweep.

Fig. 8a shows cyclic voltammograms recorded for the FIS first oxidation peak at 2-MES SAM modified electrodes in the pH range from 2 to 8. As the pH increases, the voltammetric response is shifted to less positive potentials. This behavior is expected when phenolic species are responsible for the electro-activity of the compound [55]. We previously found a similar dependence with the pH for the FIS first oxidation peak at glassy carbon electrodes [18].

On the other hand, the FIS acid dissociation constants were determined by capillary zone electrophoresis. Values of $pK_{a1} = 7.27 \pm 0.09$ and $pK_{a2} = 9.44 \pm 0.07$ were obtained for the first and the second acid dissociation constants [56]. Thus, the protonated species would be the only species present in solution in the pH range from 2 to 5. At pH >5 a mixture of dissociated and non-dissociated species would be present in solution. In addition, the recorded currents are smaller than those obtained on the bare gold electrode (compare Figs. 7 and 8), indicating that the electron transfer reaction is occurring through pinholes and/or defects present in the monolayer. In addition, the definition of the complementary cathodic peak also showed a dependence on the pH. Thus, it is better defined at pH's 3–5. Moreover, a small complementary cathodic peak is also observed at pH's 2, 6, 7 and 8. Based on these results, we chose a

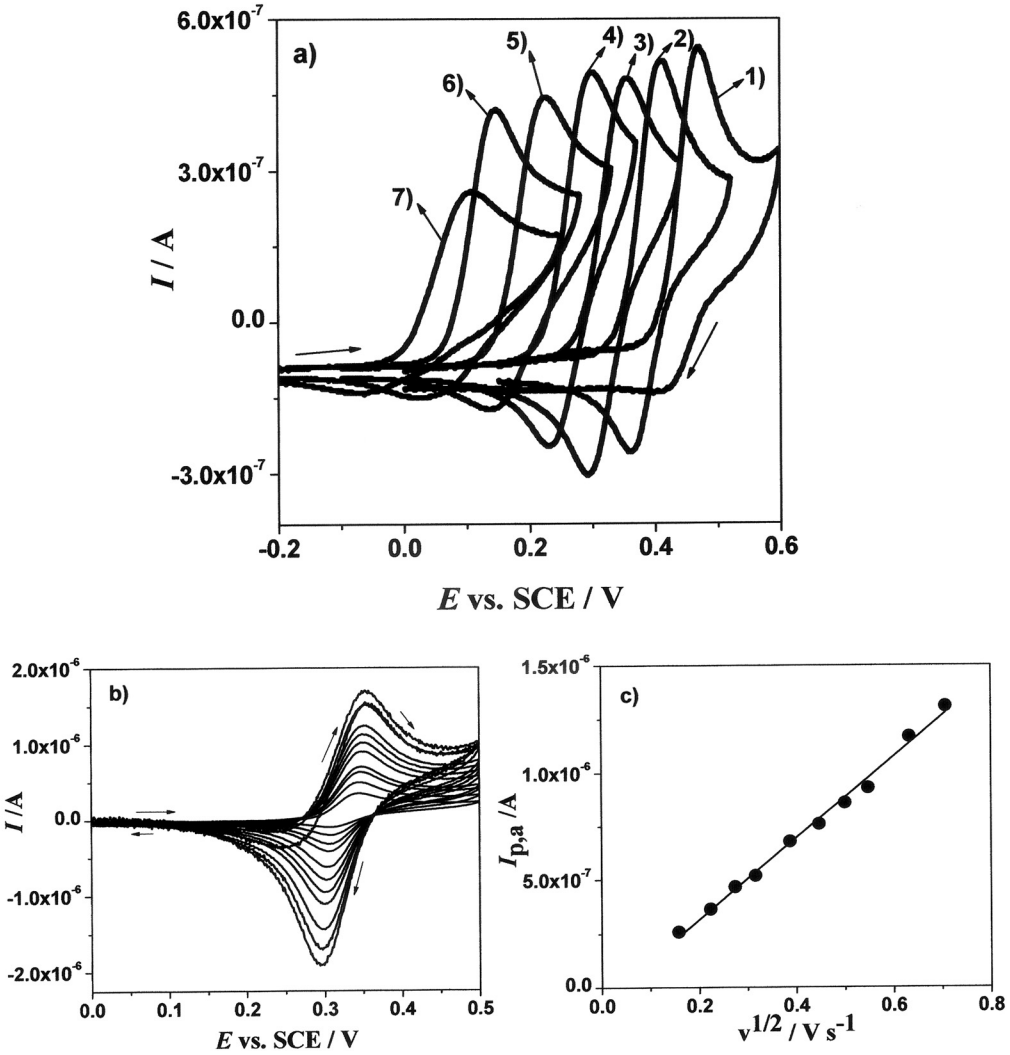

Fig. 8. a) Cyclic voltammograms of FIS at 2-MES SAM modified electrode at different pH: 1) 2.00, 2) 3.00, 3) 4.00, 4) 5.00, 5) 6.00, 6) 7.00 and 7) 8.00. v = 0.050 V s^{-1}. b) Cyclic voltammograms recorded in the scan rate range from 0.025 to 0.600 V s^{-1} at 2-MES SAM modified electrode in 15% DMSO + 85% pH 4.00 PBS. Arrows indicate the direction of potential sweep. c) A plot of the anodic peak current ($I_{p,a}$) as a function of the $v^{1/2}$. $c^*_{FIS} = 1 \times 10^{-4}$ M.

pH 4 for further studies. This pH value was chosen because the redox couple shows a slightly greater reversibility at pH 4 than at pH 3 and 5.

A plot of the $E_{p,a}$ as a function of pH was linear (r = 0.9978) with a slope of −(0.063 ± 0.002) V/decade, indicating that the same number of electrons and protons is involved in the electrode process [57].

Fig. 8b shows cyclic voltammograms recorded at pH 4 for the FIS first oxidation peak in the scan rate range from 0.025 to 0.600 V s^{-1}. Plots of $I_{p,a}$ vs. $v^{1/2}$ were linear (Fig. 8c). These findings show that the electrode process is controlled by diffusion [38]. In addition, the separation between anodic and cathodic peak potentials, ΔE_p, was (0.035 ± 0.001) V in the scan rate range from 0.025 to 0.150 V s^{-1} indicating that the exchanged electron numbers is 2 [38]. Moreover, when the electrode was transferred to a blank solution after recording cyclic voltammograms in the presence of FIS no voltammetric signal was observed, indicating that the adsorption process is negligible. These findings would indicate that monolayers contain either many closely spaced small pinholes, or a few large pinholes, giving rise to the typical voltammetric signals controlled by diffusion [58].

3.3.2. 4-MP SAM

Fig. 9 shows FIS cyclic voltammograms recorded at 4-MP modified gold electrodes in 15% DMSO + 85% pH 4.00 PBS. A quasi-reversible redox couple is also found for the FIS first oxidation peak, with a $E_{p,a}$ at about 0.375 V (line 2 in Fig. 9). The voltammetric signal stabilization was also obtained after three successive sweeps. A similar voltammetric signal was obtained in a blank solution (15% DMSO + 85% pH 4.00 PBS) when the modified electrode was previously immersed in a FIS solution for a given time (t = 5 min), but with currents lower than those obtained in the presence of FIS (line 3 in Fig. 9). Voltammetric responses were highly reproducible on successive scans. This behavior shows that FIS is adsorbed at the surface of this modified electrode. On the other hand, studies related to the dependence of $I_{p,a}$ with v demonstrated that the electrode process in FIS solutions shows a diffusion/adsorption mixed control [59].

Based on these results, we studied the surface redox couple in blank solutions (15% DMSO + 85% pH 4.00 PBS). Thus, the surface coverage (Γ) was determined from Eq. (1) [38], where Q is the charge under the oxidation ($Q_{FIS,\ red}$) or the reduction ($Q_{FIS,ox}$) peaks of the FIS surface redox couple, A is the microscopic electrode area, F was previously defined and n the exchanged electron number, i.e., n = 2.

Values of $\Gamma_{FIS,red}$ and $\Gamma_{FIS,ox}$ of (2.0 ± 0.2) × 10^{-12} mol cm^{-2} and (2.4 ± 0.2) × 10^{-12} mol cm^{-2}, respectively, were obtained for

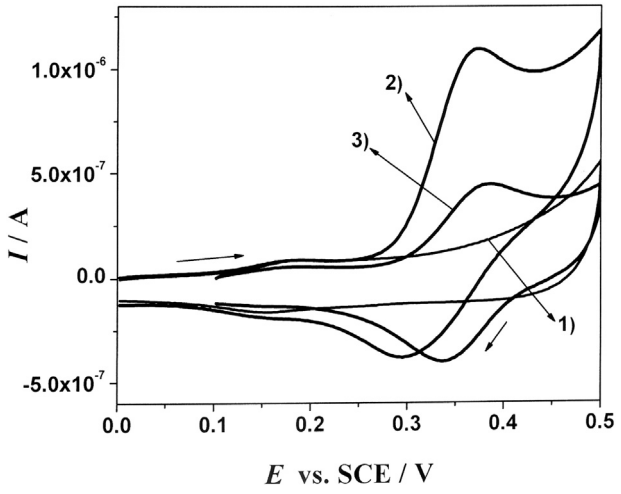

Fig. 9. Cyclic voltammograms recorded in 15% DMSO + 85% pH 4.00 PBS at 4-MP SAM modified electrode in: the blank solution (line 1); in the presence of FIS (line 2), and in the blank solution after immersing the modified electrode in the FIS solution during 5 min (line 3). c^*_{FIS} = 1.9 × 10^{-4} M. v = 0.050 V s^{-1}. Arrows indicate the direction of potential sweep.

1 × 10^{-6} M FIS bulk concentration. These values are lower than those expected for a monolayer of adsorbed substrate [38]. This behavior can be explained considering that the FIS adsorption occurs in pinholes and/or defects of the monolayer. The specific interaction of both FIS and its oxidation product (FIS, ox) with 4-MP-SAM modified electrode could be explained considering the presence of phenolic groups in both FIS (Fig. 1) and 4-MP.

3.3.3. Analytical application

It is well known that SWV is an effective and rapid electroanalytical technique, because it is able to discriminate against background currents, and diminish the limit of detection (LOD) [60,61].

The net anodic peak currents ($I_{p,n}$) of SW voltammograms of FIS in 15% DMSO + 85% pH 4.00 PBS at 2-MES-SAM modified electrode were obtained in the concentration range from 1 × 10^{-7} to 1 × 10^{-4} M (Fig. 10a). The linear regression between $I_{p,n}$ and c^*_{FIS} could be expressed by least-square procedure as:

$$I_{p,n}(A) = (0.027 \pm 0.001)\ c^*_{FIS}(M) + (10 \pm 5)\ x\ 10^{-8}(A) \quad r = 0.9919 \tag{8}$$

The lowest concentration measured experimentally for a 3:1 signal to noise ratio was 5 × 10^{-8} M (14.3 ppb). Reproducibility was determined from measurements made with four different modified electrodes. Thus, from slopes of the calibration curves a percent relative standard deviation (RSD %) of 2.2% was obtained. The repeatability was determined from five calibration curves obtained with the same modified electrode. From slopes of calibration curves, a RSD % = 0.5% was calculated.

On the other hand, and considering the surface nature of FIS redox couple at 4-MP-SAM modified electrodes, we studied which was the best potential (E_{acc}) and the accumulation time (t_{acc}) to perform the calibration curves. Thus, the E_{acc} was varied from −0.100 to 0.100 V vs. SCE. We found that there were no significant changes in current responses with the E_{acc}. However, the current response was higher when an E_{acc} was applied compared with those obtained at open circuit potential. Therefore, an E_{acc} = 0.1 V was used. In addition, the t_{acc} was varied from 10 to 900 s. We found that the current increased with increasing t_{acc}, but almost constant current values were obtained for $t_{acc} \geq 900$ s. Thus, t_{acc} = 900 s was chosen as the best to carry out the calibration curve. The linear range was from 1 × 10^{-6} to 1 × 10^{-5} M (Fig. 10b). The calibration curve can be expressed by least-square procedure as:

$$I_{p,n}\ (A) = (0,063 \pm 0,001)\ c^*_{FIS}(M) + (1,8 \pm 0,8)\ x\ 10^{-8} \quad r = 0.9988 \tag{9}$$

The lowest concentration measured experimentally for a signal to noise ratio of 3:1 was 5 × 10^{-7} mol L^{-1} (143 ppb). The reproducibility was 1.6%. We found that a modified electrode could be used again if it left a period of about 20 min in the blank solution (15% DMSO + 85% pH 4.00 PBS). Thus, the repeatability was 1.3%.

4. Conclusions

We discuss the fisetin first electrochemical oxidation peak at gold electrodes modified with 2-mercaptoethanesulphonic acid and 4-mercaptophenol self-assembled monolayers in 15% dimethylsulfoxide + 85% phosphate buffer solutions of different pH.

The monolayers were characterized by reductive desorption, electrochemical impedance spectroscopy, contact angle measurements, and the determination of the apparent surface pKa.

Both thiols form monolayers with a relatively high coverage and with a perpendicular orientation to the electrode surface, but with a low degree of packing, which is expected to short-chain thiols.

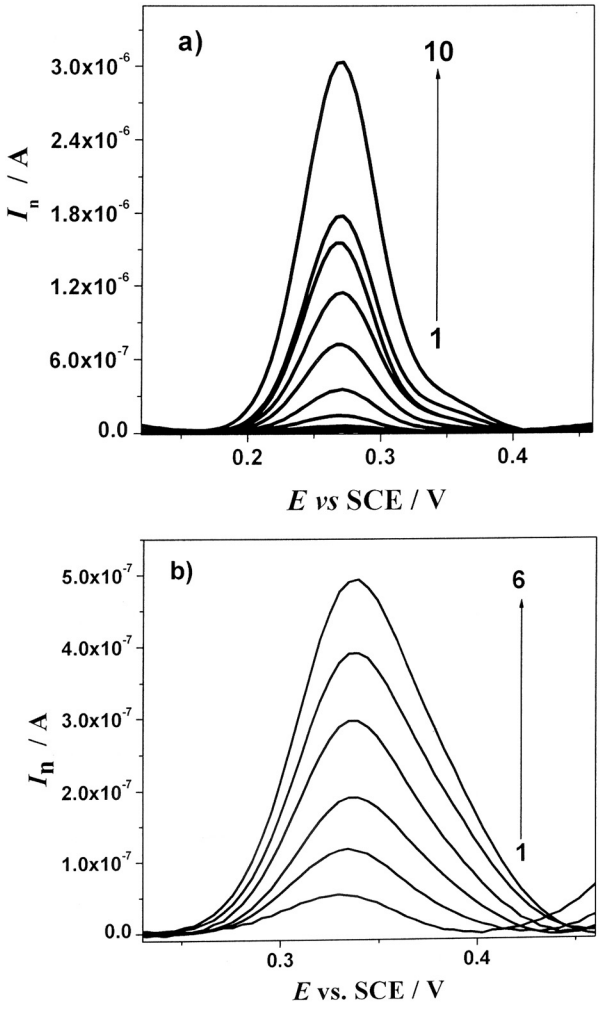

Fig. 10. Square wave voltammograms recorded in 15% DMSO + 85% pH 4.00 PBS at different FIS bulk concentrations at a) the 2-MES SAM modified electrode. The c^*_{FIS} was from 1 to 10: 1×10^{-7}, 5×10^{-7}, 1.1×10^{-6}, 5×10^{-6}, 1.1×10^{-5}, 2.1×10^{-5}, 3.5×10^{-5}, 5×10^{-5}, 6×10^{-5} and 1.1×10^{-4} M, and b) at the 4-MP SAM modified electrode obtained as it is described in Section 3.3.2, where c^*_{FIS} was from 1 to 6: 1×10^{-6}, 2×10^{-6}, 4×10^{-6}, 6×10^{-6}, 8×10^{-6} and 1×10^{-5} M. $\Delta E_{SW} = 0.025$ V, $\Delta E_s = 0.005$ V and f = 20 Hz. $E_{acc} = 0.1$ V, $t_{acc} = 900$ s.

From the apparent surface pKa values, we could infer that the 2-mercaptoethanesulphonic acid is deprotonated at all pH, generating a modified surface with a negative charge. This negative charge would prevent fisetin adsorption at this modified electrode, giving rise to a diffusion controlled and highly reproducible electrochemical response.

On the other hand, values for the apparent surface pKa of 9.76 and 9.1 were determined for 4-mercaptophenol monolayer from cyclic voltammetry and angle contact measurements, respectively, indicating that at pH 4 the monolayer is protonated. The presence of the phenolic group on the electrode surface would be responsible for fisetin adsorption on this modified electrode.

These modified electrodes were also used to perform the fisetin electroanalytical determination using the commercial reagent.

Acknowledgements

Financial supports from Agencia Nacional de Promoción Científica y Tecnológica (FONCYT) (PICT 0916/2010), Consejo Nacional de Investigaciones Científicas y Técnicas (CONICET) (PIP 112-201101-00184), Ministerio de Ciencia y Tecnología de la Provincia de Córdoba (MINCyT) (PID 050/2010), and Secretaría de Ciencia y Técnica (SECyT) (PPI 2012–2015, Res. 328/12) from Universidad Nacional de Río Cuarto are gratefully acknowledged. E. Maza thanks to CONICET for a doctoral fellowship. We thank Professor Diego Acevedo for helping us to perform contact angle measurements. We thank to Reviewers by their valuable suggestions.

References

[1] E. Grotewold (Ed.), The Science of Flavonoids, Springer, New York, 2006.
[2] P. Greenwald, C.K. Clifford, J.A. Milner, Eur. J. Cancer 37 (2001) 948–965.
[3] J.Y. Kim, Y.K. Jeon, W. Jeon, M.J. Nam, Food Chem. Toxicol. 48 (2259) (2010) 2264.
[4] H.H. Park, S. Lee, J.M. Oh, M.-S. Lee, K.-H. Yoon, B.H. Park, J.W. Kim, H. Song, S.-H. Kim, Pharmacol. Res. 55 (2007) 31–37.
[5] R.N. Puri, R.W. Colman, Anal. Biochem. 210 (1993) 50–57.
[6] B. Sengupta, A. Banerjee, P.K. Sengupta, FEBS Lett. 570 (2004) 77–81.
[7] R.I. Brinkworth, M.J. Stoermer, D.P. Fairlie, Biochem. Biophys. Res. Commun. 188 (1992) 631–637.
[8] B. Sengupta, J. Swenson, Biochem. Biophys. Res. Commun. 334 (2005) 954–959.
[9] P. Maher, Genes Nutr. 4 (2009) 297–307.
[10] I. Molnar-Perl, Z. Füzfai, J. Chromatogr. A 1073 (2005) 201–227.
[11] L.-Z. Lin, J.M. Harnly, J. Agric, Food Chem. 55 (2007) 1084–1096.
[12] A.M. Danila, A. Kotani, H. Hakamata, F. Kusu, J. Agric, Food Chem. 55 (2007) 1139–1143.
[13] G.J. Volikakis, C.E. Efstathiou, Talanta 51 (2000) 775–785.
[14] W.F. Hodnick, E.B. Milosavljevic, J.H. Nelson, R.S. Pardini, Biochem. Pharmacol. 37 (1988) 2607–2611.
[15] H.P. Hendrickson, A.D. Kaufman, C.E. Lunte, J. Pharm. Biomed. Anal. 12 (1994) 325–334.
[16] H.P. Hendrickson, M. Sahafayen, M.A. Bell, A.D. Kaufman, M.E. Hadwiger, C.E. Lunte, J. Pharm. Biomed. Anal. 12 (1994) 335–341.
[17] A.M. Olivera Brett, M.E. Ghica, Electroanalysis 15 (2003) 1745–1750.
[18] E.M. Maza, M.B. Moressi, H. Fernández, M.A. Zón, J. Electroanal. Chem. 675 (2012) 11–17.
[19] H.O. Finklea, Electrochemistry of organized monolayers of thiols and related molecules on electrodes, in: A.J. Bard, I. Rubinstein (Eds.), Electroanalytical Chemistry, vol. 19, Marcel Dekker, New York, 1996.
[20] P. Ramírez, R. Andreu, J.J. Calvente, C.J. Calzado, G. López-Pérez, J. Electroanal. Chem. 582 (2005) 179–190.
[21] F. Li, L. Tang, W. Zhou, Q. Guo, Langmuir 26 (2010) 9484–9490.
[22] L. Srisombat, A.C. Jamison, T.R. Lee, Colloids Surf. A Physicochem. Eng. Asp. 390 (2011) 1–19.
[23] C.R. Raj, T. Ohsaka, J. Electroanal. Chem. 496 (2001) 44–49.
[24] P. Ihalainen, H. Majumdar, A. Määttänen, S. Wang, R. Österbacka, J. Peltonen, Biochim. Biophys. Acta 1830 (2013) 4391–4397.
[25] M.B. Moressi, R. Andreu, J.J. Calvente, H. Fernández, M.A. Zón, J. Electroanal. Chem. 570 (2004) 209–217.
[26] M.B. Moressi, J.J. Calvente, R. Andreu, H. Fernández, M.A. Zón, J. Electroanal. Chem. 605 (2007) 118–124.
[27] D. Mandler, S. Kraus-Ophir, J. Solid State, Electrochemistry 15 (2011) 1535–1558.
[28] L.A. Hockett, S.E. Creager, Langmuir 11 (1995) 2318–2321.
[29] K. Motesharei, D.C. Myles, J. Am. Chem. Soc. 116 (1994) 7413–7414.
[30] C.H. Shen, J.C. Lin, Colloids Surf. B 101 (2013) 376–383.
[31] D.T. Sawyer, A. Sobkowiak, J.L. Roberts, Electrochemistry for Chemists, second ed. J. Wiley & Son, New York, USA, 1995.
[32] E. Gileadi, E. Kirowa-Eisner, J. Penciner, Interfacial Electrochemistry – An Experimental Approach, Addison-Wesley, Reading, MA, 1975.
[33] C.A. Widrig, C. Chung, M.D. Porter, J. Electroanal. Chem. 310 (1991) 335–359.
[34] W. Wang, S. Zhang, P. Chinwangso, R.C. Advincula, T.R. Lee, J. Phys. Chem. C 113 (2009) 3717–3725.
[35] M.J. Esplandiu, H. Hagenström, D.M. Kolb, Langmuir 17 (2001) 828–838.
[36] H. Munakata, D. Oyamatsu, S. Kuwabata, Langmuir 20 (2004) 10123–10128.
[37] M.L. Carot, M.J. Esplandiu, F.P. Cometto, E.M. Patrito, V.A. Macagno, J. Electroanal. Chem. 579 (2005) 13–23.
[38] A.J. Bard, L.R. Faulkner, Electrochemical Methods: Fundamentals and Applications, second ed. Marcel Dekker, New York, 2001.
[39] T.F. Paulo, H.D. Abruña, I.C.N. Diógenes, Langmuir 28 (2012) 17825–17831.
[40] N.K. Chaki, M. Aslam, J. Sharma, K. Vijayamohanan, Proc. Indian Acad. Sci. 113 (2001) 659–670.
[41] S. Campuzano, M. Pedrero, C. Montemayor, E. Fatás, J.M. Pingarrón, J. Electroanal. Chem. 586 (2006) 112–121.
[42] F. Pak, K. Meral, R. Altundaş, D. Ekinci, J. Electroanal. Chem. 654 (2011) 20–28.
[43] M.L. Carot, V.A. Macagno, P. Paredes-Olivera, E.M. Patrito, J. Phys. Chem. C 111 (2007) 4294–4304.
[44] E. Boubour, R.B. Lennox, Langmuir 16 (2000) 7464–7470.
[45] L.V. Protsailo, W.R. Fawcett, Electrochim. Acta 45 (2000) 3497–3505.
[46] T. Kakiuchi, M. Iida, S.I. Imabayashi, K. Niki, Langmiur 16 (2000) 5397–5401.
[47] Z. Dai, H. Ju, Phys. Chem. Chem. Phys. 3 (2001) 3769–3773.
[48] S.C. Burris, Y. Zhou, W.A. Maupin, A.J. Ebelhar, M.W. Daugherty, J. Phys. Chem. C 112 (2008) 6811–6815.
[49] J. Zhao, L. Luo, X. Yang, E. Wang, S. Dong, Electroanalysis 11 (1999) 1108–1111.
[50] A.M. Collieu, D.J. Powney, The Mechanical and Thermal Properties of Materials, Ed. Reverté, 1977.
[51] Y.C. Jung, B. Bhushan, Nanotechnology 17 (2006) 4970–4980.
[52] A. Maho, J. Denayer, J. Delhalle, Z. Mekhalif, Electrochim. Acta 56 (2011) 3954–3962.

[53] S.E. Creager, J. Clarke, Langmuir 10 (1994) 3675–3683.
[54] D. Nematollahi, M. Malakzadeh, J. Electroanal. Chem. 547 (2003) 191–195.
[55] O. Hammerich, B. Svensmark, in: H. Lund, M.M. Baizer (Eds.), Organic Electrochemistry: An Introduction and a Guide, third ed.Marcel Dekker, New York 1990, p. 616.
[56] J.M. Herrero-Martínez, M. Sanmartín, M. Rosés, E. Bosch, C. Râfois, Electrophoresis 26 (2005) 1886–1895.
[57] M. Heyrovský, S. Vavricka, J. Electroanal. Chem. 36 (1972) 203–221.
[58] C. Amatore, J.M. Saveant, D. Tessier, J. Electroanal. Chem. 147 (1983) 39–51.
[59] B.E. Conway, D.C.W. Kannagara, J. Electrochem. Soc. 134 (1987) 906–918.
[60] K.B. Oldham, J.C. Myland, Fundamentals of Electrochemical Science, Academic Press, San Diego, California, 1994.
[61] V. Mirceski, S. Komorsky-Lovric, M. Lovric, Square Wave Voltammetry Theory and Application, Springer, Leipzig, Germany, 2007.